

Solution of Real Magnetogasdynamics Equations using a TVD Scheme as a Tool for Electric Propulsion¹

***⁺Sergio A. Elaskar and ⁺Héctor H. Brito**

**Departamento de Aeronáutica, Universidad Nacional de Córdoba
Av. Velez Sarfield 1601, Córdoba (5000), Argentina*

*⁺Centro de Investigaciones Aplicadas, Instituto Universitario Aeronáutico
Ruta 20, km. 5.5, Córdoba (5022), Argentina*

e-mail: selaskar@com.uncor.edu

e-mail: hbrito@make.com

IEPC-01-161

The main objective of this work is to present the results obtained with a computational code which solves the real magnetogasdynamic equations (MGD). This research is the initial stage towards achieving a comprehensive description of the ablative pulse plasma thruster (APPT) behavior. The equations that govern MGD flows are continuity, momentum, energy and magnetic induction together with a state equation. These equations have two parts: the first one contains the conservation terms and is hyperbolic; the second one has the diffusive terms and is parabolic. The parabolic part of the equations is written in divergence form, so that there is a diffusive flux. The numerical approach consists of an approximate Riemann solver together with the TVD scheme proposed by Yee. The “eigensystem” technique presented by Powell has also been used and the eigenvectors normalization has been carried out. To check the accuracy of the computational code a Riemann problem introduced by Brio and Wu has been simulated. The obtained results are in close agreement with those reported by other authors.

Introduction

The main objective of this work is to present the results obtained with a computational code developed to solve the solution of real magnetogasdynamic equations (MGD). This research represents the initial stage towards achieving a comprehensive description of the APPT behavior. There are previous works in which the authors use or develop numerical codes to simulate

the flow inside of magnetoplasma dynamics thruster. For example two-dimensional codes have been developed by Toki *et al.* [12], and Ao and Fujiwara [1]. Effects of the geometry on the performances has been studied by LaPointe [5], and Mikellides and Turchi [6] using the codes MACH2 and MACH3 to simulate the non-steady flow in two and three dimensions. None of these works apply techniques classically used in fluid mechanics that allow for the high resolution capture of

¹ Copyright © 2001 by the Electric Rocket Propulsion Society

discontinuities. The present research explores the capacity of these techniques to simulate the plasma flow.

Sankaran and Choueiri.[9,10] are using a procedure similar to that described in this research, however the numerical techniques are fairly different.

The equations that govern MGD flows are continuity, momentum, energy and magnetic induction together with a state equation. These equations form a hyperbolic-parabolic system, see Sankaran, *et al.* [9]. The hyperbolic terms represent the ideal MGD equations, whilst the diffusive effects are accounted for in the parabolic terms.

A numerical technique is used which consists of an approximate Riemann solver that calculates the variables inside each cell by evaluating the flux through the contour of the cells. The TVD scheme proposed by Yee, *et al.* [13] is used to evaluate the numerical flux. The ‘‘eigensystem’’ technique presented by Powell has also been used and eigenvectors normalization has been carried out following the works of Zarachay *et al.* [14], Roe and Balsara [8], and Bodgan [2]. To check the accuracy of the computational code a Riemann problem introduced by Brio and Wu [3] has been simulated. The parabolic components are written in conservation form and they are considered as fluxes. To obtain the numerical flux of the parabolic contributions, the finite differences technique is used.

Plasma flow

In many situations the plasma flow can be represented by the equations of the magnetogasdynamic (Dendy, [4]). In this section these equations are introduced.

Equations of the real MGD

The equations of ideal MGD in conservative form are expressed non-dimensionally as:

$$\frac{\partial U}{\partial t} + \frac{\partial F_h}{\partial x} = \frac{\partial F_p}{\partial x} \quad (1)$$

where U is the conservative state variable vector

$$U = (\rho, \rho u_x, \rho u_y, \rho u_z, B_x, B_y, B_z, E)^T \quad (2)$$

and F_h is the vector that specifies the hyperbolic fluxes; it can be written for one dimensional problems as:

$$F_h = \begin{pmatrix} \rho u_x \\ \rho u_x^2 - B_x^2 + p + \frac{B^2}{2} \\ \rho u_x u_y - B_x B_y \\ \rho u_x u_z - B_x B_z \\ 0 \\ u_x B_y - u_y B_x \\ u_x B_z - u_z B_x \\ \left(E + p + \frac{B^2}{2} \right) u_x - (u_x B_x + u_y B_y + u_z B_z) B_x \end{pmatrix} \quad (3)$$

the density is indicated as ρ ; u_x, u_y, u_z are the components of the vector velocity; B_x, B_y, B_z represent the components of the vector magnetic field; p is the pressure; B^2 is defined as:

$$B^2 = B_x^2 + B_y^2 + B_z^2 \quad (4)$$

The energy is expressed as:

$$E = \frac{P}{\gamma - 1} + \frac{1}{2} \rho (u_x^2 + u_y^2 + u_z^2) + \frac{1}{2} (B_x^2 + B_y^2 + B_z^2) \quad (5)$$

where γ is the ratio of specific heats

The parabolic fluxes for one dimensional problems are given by:

$$F_p = \begin{pmatrix} 0 \\ \frac{4}{3} \frac{\mu}{Re Al} \frac{\partial v_x}{\partial x} \\ \frac{\mu}{Re Al} \frac{\partial v_y}{\partial x} \\ \frac{\mu}{Re Al} \frac{\partial v_z}{\partial x} \\ 0 \\ \frac{\eta_z}{Lu Al} \frac{\partial B_y}{\partial x} \\ \frac{\eta_y}{Lu Al} \frac{\partial B_z}{\partial x} \\ \frac{1}{Lu Al} \left(\frac{\eta_z}{2} B_y^2 + \frac{\eta_y}{2} B_z^2 \right) + \frac{\kappa}{Pe Al} \frac{\partial T}{\partial x} + \frac{\mu}{Re Al} \frac{\partial \left(\frac{2}{3} v_x + \frac{1}{2} v_y + \frac{1}{2} v_z \right)}{\partial x} \end{pmatrix} \quad (6)$$

where η_x, η_y, η_z are the non-dimensional resistivities, κ is the non-dimensional thermal conductivity and μ is the non-dimensional viscosity. Lu , Re and Pe are the Lunquist, Reynolds and Peclet numbers respectively.

$$\frac{\partial U}{\partial t} + A_c \frac{\partial U}{\partial x} = 0; \quad A_c = \frac{\partial F_h}{\partial U} \quad (7)$$

The hyperbolic terms system of equations (1) can be recast in their quasi-linear form:

where A_c is the flux Jacobian, the letter ‘‘c’’ indicates that the derivation has been carried out

with regard to the conservative state variables. However, the form of the flux Jacobian is simpler as a function of the primitive variables (W):

$$W = (\rho, u_x, u_y, u_z, B_x, B_y, B_z, p)^T \quad (8)$$

Therefore, Eq. (8) can be rewritten in the following way:

$$\frac{\partial U}{\partial t} + A_p \frac{\partial W}{\partial x} = 0; \quad A_p = \frac{\partial F_h}{\partial W} \quad (9)$$

The transformation rule between the Jacobian fluxes is:

$$\lambda_e = u_x; \quad \lambda_a = u_x \pm c_a; \quad \lambda_f = u_x \pm c_f; \quad \lambda_s = u_x \pm c_s; \quad \lambda_d = u_x \quad (11)$$

The Alfvén and the slow and fast magnetosonic velocities are, respectively:

$$c_a = \frac{B_x}{\sqrt{\rho}}; \quad c_{f,s}^2 = 0.5 \left[\frac{\mathcal{P} + B^2}{\rho} \pm \sqrt{\left(\frac{\mathcal{P} + B^2}{\rho} \right)^2 - 4 \frac{\mathcal{P} B_x^2}{\rho^2}} \right] \quad (12)$$

where the positive sign corresponds to fast magnetosonic waves.

Finally, the eigenvectors have been normalized to avoid problems due to the system degeneracy.

$$A_p = \left(\frac{\partial U}{\partial W} \right)^{-1} A_c \left(\frac{\partial U}{\partial W} \right) \quad (10)$$

Riemann solvers based on a system of eight waves using the matrix A_p cannot be applied because an eigenvalue is zero and lacks of physical meaning. It is important to notice that the formulations in primitive variables and in conservative variables are equivalent, therefore this null eigenvalue appears in both formulations. To solve this inconvenient an alternative flux Jacobian has been implemented (A'_p), as presented by Powell [7]. It is important to note that one-dimensional problems do not require to use this new matrix. It has nevertheless been implemented in this work because this matrix allows for a straightforward extension to simulations in two or three dimensions. The eigenvalues of the matrix A'_p are:

Transport coefficients

To evaluate the viscosity (μ), electric conductivity (σ) and thermal conductivity (κ) the expressions given by Spitzer [11] are used:

$$\begin{aligned} \mu &= 2.204 \times 10^{-14} \frac{M_i T^{\frac{5}{2}}}{Z^2 \ln \Lambda}, \\ \sigma &= 2.634 \times 10^{-2} \gamma_E(Z) \frac{T^{\frac{3}{2}}}{z \ln \Lambda}, \\ \kappa &= 1.96 \times 10^{-9} \varepsilon_T(Z) \delta_T(Z) \frac{T^{\frac{5}{2}}}{z \ln \Lambda} \end{aligned} \quad (13)$$

where M_i is the atomic number of the ions in the plasma, T is the temperature, z is the mean ion charge, Λ and is the number of particles in a Deybe

sphere. Coefficients $\varepsilon_T(Z)$, $\delta_T(Z)$ and $\gamma_E(Z)$ are correction factors; when $z=1$ the coefficients are $\gamma_E(Z)=0.582$, $\varepsilon_T(Z)=0.419$ and $\delta_T(Z)=0.225$.

Numerical method

Eq. (6) is a hyperbolic-parabolic system, so that hyperbolic (conservative) and parabolic (dissipative) fluxes appear in it. The solution of Eq. (6) must take into account both contributions.

To reach the numerical solution of Eq. (6), a time linearization of the system is employed. This technique permits to calculate the hyperbolic numerical fluxes, the parabolic numerical fluxes and the total numerical fluxes as the sum of both.

The TVD numerical scheme used to solve the hyperbolic part is presented in first place. The parabolic part is evaluated by conventional finite differences.

Hyperbolic contribution

The equations outlined in the previous section are solved using an approximate Riemann solver together with an explicit scheme. To calculate the numerical flux the TVD upwind technique of Yee, *et al.* [13] has been implemented, by doing so a second order approach is obtained. This technique is used to calculate the numerical fluxes in all interior cells. The TVD method for the system given in Eq. (1) can be expressed in the following way:

$$U_j^{n+1} = U_j^n - \frac{\Delta t}{\Delta x} \left(\bar{F}_{j+\frac{1}{2}}^n - \bar{F}_{j-\frac{1}{2}}^n \right) \quad (15)$$

The function that determines the numerical fluxes is defined as:

$$\bar{F}_{j+\frac{1}{2}}^n = \frac{1}{2} \left(F_{j+1}^n + F_j^n + R_{j+\frac{1}{2}}^n \Phi_{j+\frac{1}{2}}^n \right)_h + \left(F_{j+\frac{1}{2}}^n \right)_p \quad (16)$$

being R the matrix that contains the right eigenvectors of the matrix A_C . Φ is the dissipation vector whose elements for the second order TVD-upwind scheme are expressed by:

$$\phi_{j+\frac{1}{2}}^l = (g_{j+1}^l + g_j^l) - \sigma \left(\lambda_{j+\frac{1}{2}}^l + \gamma_{j+\frac{1}{2}}^l \right) \alpha_{j+\frac{1}{2}}^l \quad (17)$$

The following limiter function was used in this work:

$$g_j^l = \text{sgn} \left(\lambda_{j+\frac{1}{2}}^l \right) \max \left\{ 0, \min \left[\sigma_{j+\frac{1}{2}}^l \left| \alpha_{j-\frac{1}{2}}^l \right|, \frac{\text{sgn} \left(\lambda_{j+\frac{1}{2}}^l \right)}{2} \sigma_{j+\frac{1}{2}}^l \left| \alpha_{j-\frac{1}{2}}^l \right| \right] \right\} \quad (18)$$

The function $\sigma(z)$ is given by:

$$\begin{aligned} \sigma(z) &= |\lambda|, & \text{if } |\lambda| \geq \varepsilon \\ \sigma(z) &= \frac{\lambda^2 + \varepsilon^2}{2\varepsilon}, & \text{if } |\lambda| < \varepsilon \end{aligned} \quad (19)$$

For the sake of simplicity, the primitive variables have been used to obtain α^l :

$$\alpha^l = L_p^l \cdot (W_{i+1} - W_i) \quad (21)$$

and $\gamma_{j+\frac{1}{2}}^l$ is defined as:

$$\begin{aligned} \gamma_{j+\frac{1}{2}}^l &= \frac{(g_{j+1}^l - g_j^l)}{\alpha_{j+\frac{1}{2}}^l}, & \text{if } \alpha_{j+\frac{1}{2}}^l \neq 0 \\ \gamma_{j+\frac{1}{2}}^l &= 0, & \text{if } \alpha_{j+\frac{1}{2}}^l = 0 \end{aligned} \quad (20)$$

L_p^l being the left eigenvector of the l^{th} wave.

Parabolic contribution

A discretization scheme of the parabolic flux is introduced in this section. A conventional finite difference technique is employed.

Because only one-dimension problems are considered, the parabolic contribution for the magnetic field, energy and momentum can be written as:

$$(B_y)_i^{n+1} = (B_y)_i^n + \frac{\Delta t}{(\Delta x)^2} \frac{\eta_z}{Lu} \frac{1}{Al} \left[(B_y)_{i+1}^n - 2(B_y)_i^n + (B_y)_{i-1}^n \right] \quad (22)$$

$$\begin{aligned} E_i^{n+1} &= E_i^n + \frac{\Delta t}{\Delta x} \left\{ \frac{\eta_z}{4Lu} \frac{1}{Al} \left[(B_y^2)_{i+1}^n - (B_y^2)_{i-1}^n \right] + \frac{\eta_y}{4Lu} \frac{1}{Al} \left[(B_z^2)_{i+1}^n - (B_z^2)_{i-1}^n \right] \right\} + \\ &\quad + \frac{\Delta t}{(\Delta x)^2} \frac{\kappa_x}{Pe} \frac{1}{Al} \left[T_{i+1}^n - 2T_i^n + T_{i-1}^n \right] + \\ &\quad + \frac{\Delta t}{(\Delta x)^2} \frac{\mu}{Re} \frac{1}{Al} \left\{ \frac{2}{3} \left[(v_x^2)_{i+1}^n - 2(v_x^2)_i^n + (v_x^2)_{i-1}^n \right] + \frac{1}{2} \left[(v_y^2)_{i+1}^n - 2(v_y^2)_i^n + (v_y^2)_{i-1}^n \right] + \frac{1}{2} \left[(v_z^2)_{i+1}^n - 2(v_z^2)_i^n + (v_z^2)_{i-1}^n \right] \right\} \end{aligned} \quad (23)$$

$$(\rho v_x)_i^{n+1} = (\rho v_x)_i^n + \frac{4}{3} \frac{\Delta t}{(\Delta x)^2} \frac{\mu}{Re} \frac{1}{Al} \left[(v_x)_i^{n+1} - 2(v_x)_i^n + (v_x)_{i-1}^n \right] \quad (24)$$

where Lu , Al , Re and Pe are the Lundquist, Alfvén, Reynolds and Peclet numbers.

Results

In this section the results obtained for the Riemann problem proposed by Brio and Wu [3] are presented. This is a benchmark widely used by the MGD scientific community with the objective of evaluating the behavior of the numerical techniques and computational codes. Brio and Wu studied the extension to MGD of the classic shock tube used in gas dynamics. This example is denominated coplanar Riemann problem because only components of the velocity and magnetic field vectors in two directions are allowed. It is important to note that Brio and Wu solved this benchmark only for ideal MGD.

The variables are given in non-dimensional form and an unit length of the magnetogasdynamic shock tube is considered. The discontinuity or diaphragm that separates the left and right initial states is located in the middle of the tube. The initial values are:

$$\begin{aligned} W_l &= (1.0, 0.0, 0.0, 0.0, 0.0, 0.75, 1.0, 0.0, 1.0)^T \\ W_r &= (0.125, 0.0, 0.0, 0.0, 0.0, 0.75, -1.0, 0.0, 0.1)^T \end{aligned} \quad (25)$$

W_l and W_r being the vectors that contain the primitive variables corresponding to both sides of the diaphragm. Figures 1, 2, 3 and 4 show the transverse magnetic field (B_y), the velocity in the longitudinal direction (u_x), the density (ρ) and the fast magnetosonic velocity plotted as a function of the longitudinal distance for ideal and real MGD. A fixed mesh with 4000 nodes is used.

Finally, one observes that the time required to simulate real MGD flows is greater than the time employed in the simulation of ideal MGD, so to keep computing times comparable, a lower number of nodes should be used. The adopted values of

viscosity, electrical resistivity and thermal conductivity are $0.00272728 Pa.s$, $0.0003 Nm^2s/C$ and $0.817 N/s^\circ K$, respectively.

It is important notice that the present numerical results agree satisfactorily with those published by Brio and Wu [3] and Bodgan [2].

Conclusions

The main conclusions obtained throughout this research are the followings:

- The numerical simulation using an approximate Riemann solver together with the Yee's TVD scheme has shown to be an effective alternative from the point of view of low computational cost and the accuracy of the results for ideal magnetogasdynamic.
- The technique developed by Powell does not introduce modifications in the results as compared to those obtained by using seven waves.
- The evaluation of the parabolic terms introduces additional constraints on the CPU time. This is larger than for the ideal MGD.
- To achieve the solution of the real magnetogasdynamics equations, CFL numbers lower than those required for the ideal magnetogasdynamics equations, must be used.
- The parabolic contributions lead to smooth distributions of the mechanical and magnetic variables. Therefore, the corresponding waves are not sharply defined.

Acknowledgement

This work has been supported by means of grants PICT-99-10-07107 of Argentina's National Agency for the Support of Science and Technology and 05-M026 of National University of Cordoba. Support

provided by a grant from Córdoba Science Agency is also acknowledged.

References

1. **Ao, T. and Fujiwara, T.**, *Numerical and experimental study of an MPD thruster*, IEPC-84-08, 1984.
2. **Bogdan, U.**, *An advanced implicit solver for MHD*, PhD Thesis, University of Washington, 1999.
3. **Brio, M. and Wu, C.**, *An upwind differencing scheme for the equations of magnetohydrodynamics*, Journal Computational Physics, Vol. 45, , 1988, pp. 400-422.
4. **Dendy, R.**, *Plasma Physics. An Introductory Course*, Cambridge University Press, Cambridge, 1999.
5. **LaPointe, M.**, *Numerical simulation of geometric scale effects in cylindrical self-field MPD thrusters*, NASA-CR-189224, 1992.
6. **Mikellides, I. and Turchi, P.**, *Optimization of pulse plasma thrusters in rectangular and coaxial geometries*, IEPC-99-211, 1999.
7. **Powell, K.**, *An approximate Riemann solver for magnetohydrodynamics (that works in more than one dimension)*, NASA Contract No NAS1-19480, ICASE, NASA Langley Research Center, Hampton, 1995.
8. **Roe, P. and Balsara, D.**, *Notes on the eigensystem of magnetohydrodynamics*, SIAM Journal Applied Mathematics, Vol. 56, 1996, pp. 57-67.
9. **Sankaran, K.; Choueiri, E. and Jardin, S.**, *Application of the new numerical solver to the simulation of the MPD flows*, AIAA-2000-3537, 2000.
10. **Sankaran, K. and Choueiri, E.**, *An accurate characteristics-splitting scheme for numerical solution of MHD equations*, IEPC-99-208, 1999.
11. **Spitzer, V.**, *Physics of fully ionized gases*, Interscience Publishers, New York, 1956.
12. **Toki, K.; Kimura, I. and Tanaka, M.**, *Current distribution on the electrodes of MPD arcjets*, AIAA Journal, Vol 20 No 7, 1982, pp 889-897.
13. **Yee, H.; Warming, R. and Harten, A.**, *Implicit total variations diminishing (TVD) schemes for steady-state calculations*, Journal Computational Physics, Vol. 57, 1985, pp. 327-360.
14. **Zarachay, A.; Malagoli, A. and Collela, P.**, *A higher order Godunov method for multidimensional ideal magnetohydrodynamics*, SIAM Journal on Scientific Computation, Vol. 15, 1994, pp. 263-284.

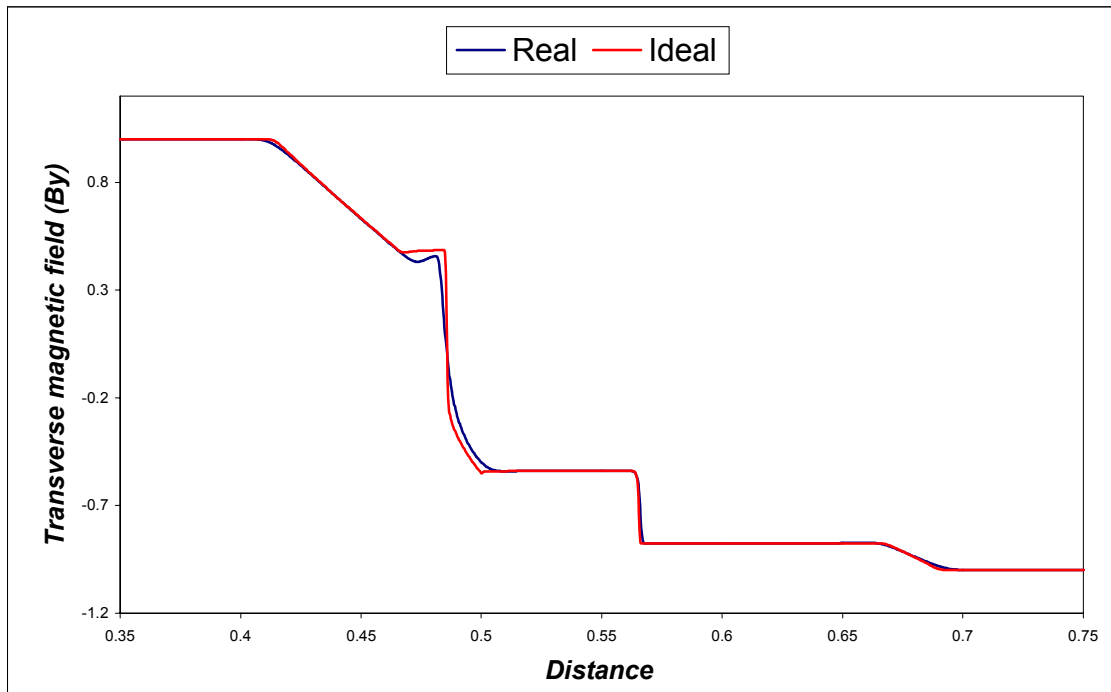


Figure 1. Transverse magnetic field as a function of the longitudinal distance.

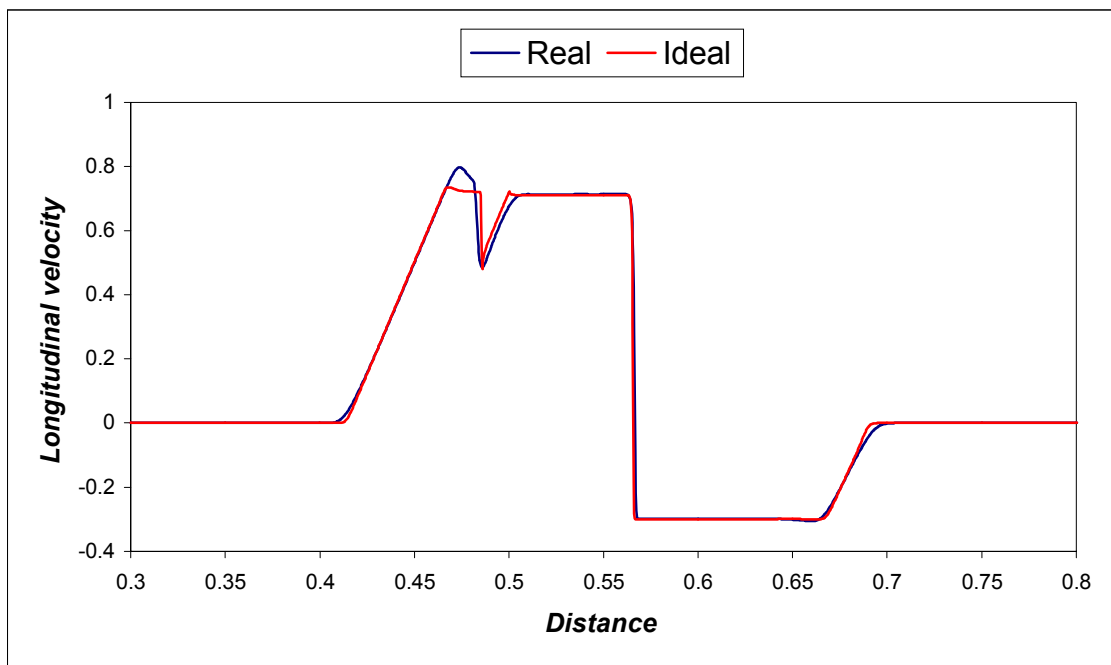


Figure 2. Longitudinal velocity as a function of the longitudinal distance.

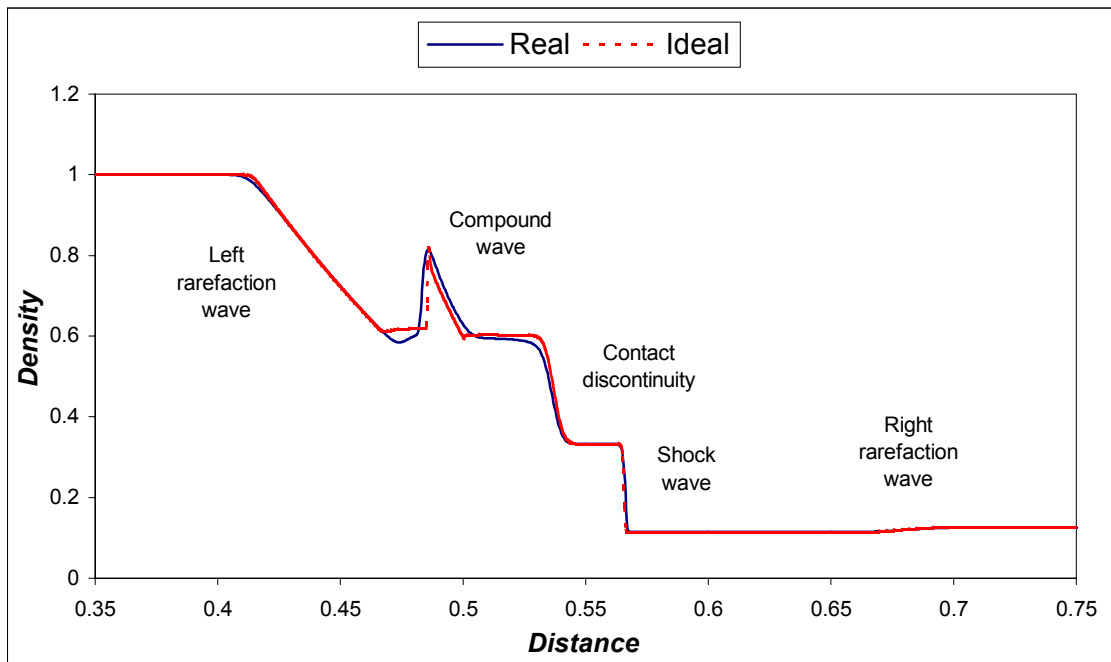


Figure 3. Density as a function of the longitudinal distance.

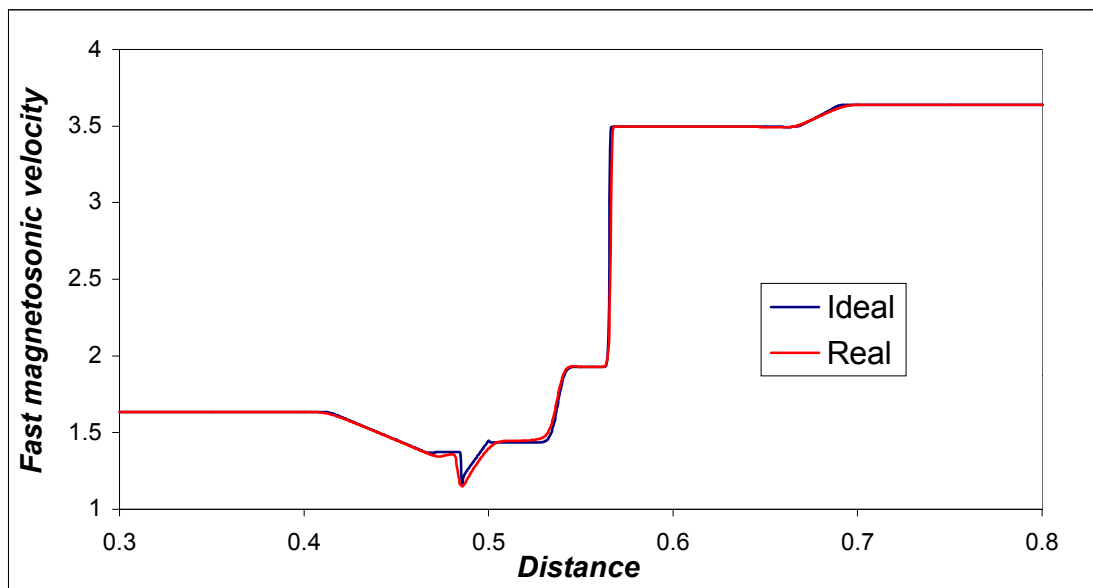


Figure 4. Fast magnetosonic velocity as a function of the longitudinal distance.